Nuclear-Magnetic-Resonance Study of Thulium Aluminum Garnet†

V. HUGO SCHMIDT
Physics Department, Montana State University, Bozeman, Montana 59715

AND

E. D. JONES
Sandia Laboratories, Albuquerque, New Mexico 87115

(Received 29 August 1969)

The Tm^{169} and the Al^{27} nuclear magnetic resonance have been studied in cubic thulium aluminum garnet. The Tm^{169} results at 1.5°K give magnetic-susceptibility tensor components of $\chi_1=0.014$, $\chi_2=0.551$, and and $\chi_3=0.030$ emu/g ion, which show much more anisotropy than found previously for thulium gallium garnet. The measured Al^{27} paramagnetic shifts at 1.5°K agree quite well with values calculated from Tm^{3+}-ion dipole sums. The Al^{27} paramagnetic shifts from 1.5 to 300°K are used to calculate the approximate temperature dependence of the Tm^{3+}-ion susceptibility components. The room-temperature Al^{27} quadrupolar coupling constants $|e^2qQ/h|$ for the axially symmetric a and d sites are 0.892 ± 0.005 and 6.155 ± 0.005 MHz, respectively. The unshielded electric field gradients are calculated and compared with corresponding values for other aluminum garnets and for Fe^{57} sites in several iron garnets. These field gradients agree quite well with values calculated using a point-charge model.

I. INTRODUCTION

RARE-EARTH garnets have received considerable attention with regard to their magnetic and optical properties and their magnetic and electric crystalline fields. The iron garnets are ferrimagnetic up to about 300°C, while the aluminum and gallium garnets generally are paramagnetic to liquid-helium temperatures. The garnet structure is cubic [space group $O_h(10)$–$1a3d$], with cation coordinates which are simple fractions of the unit-cell length, while the oxygen positions are arbitrary. Thulium aluminum garnet (TmAlG) has the chemical formula $Tm_3Al_2(AlO_4)_3$, with Al_2 corresponding to a site Al^{3+} ions located in sites having axial symmetry about nonintersecting lines which run in the ⟨111⟩ directions. The other Al^{3+} ions are in d sites which alternate with Tm^{3+} ions in nonintersecting chains which run in the ⟨100⟩ directions. Ignoring the oxygens, both ions have similar environments which would have axial symmetry. The oxygens form axially distorted tetrahedra around each d-site aluminum ion, with alternate tetrahedra having different orientations. This oxygen arrangement preserves the axial symmetry of the aluminum d site, but the orientation difference reduces the thulium sites to orthorhombic symmetry, with axes oriented as shown in Fig. 1.

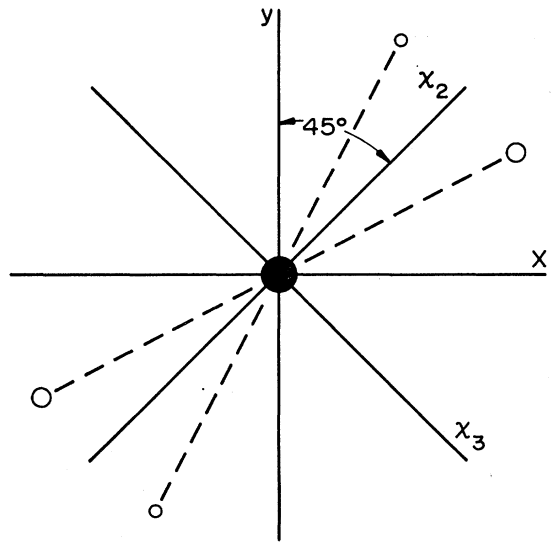

FIG. 1. Projection along z of environment of a thulium ion (filled circle) in a Tm-AlO_4-Tm···chain running along the z axis, which is the χ_1 axis for the susceptibility tensor for this thulium site. The χ_2 and χ_3 axes are oriented as shown. The large open circles are the bottom oxygens of the AlO_4 tetrahedron above the thulium ion, and the small open circles are the top oxygens of the AlO_4 below the thulium ion.

Recent Tm^{169} NMR studies[1] of the intermetallic paramagnets TmP, TmAs, and TmSb have shown that the thulium-ion effective magnetic moment has the free-ion value within experimental error. In thulium gallium garnet (TmGaG), however, the Tm^{169} NMR results[2] show that the crystalline field interaction causes the thulium ion to have an orthorhombic magnetic-susceptibility tensor which is fairly anisotropic at 4°K. The average of the tensor components agrees well with a measurement[3] of the bulk paramagnetic susceptibility, which is isotropic because of the cubic structure. The electric quadrupolar coupling constants have been measured for iron sites in iron garnets by Mössbauer studies,[4] and for aluminum sites in several aluminum garnets employing Al^{27} NMR.[5,6]

† Work supported by the U. S. Atomic Energy Commission and the National Science Foundation.

[1] E. D. Jones, Phys. Rev. Letters **19**, 432 (1967); Proc. Coll. Internat. les Elements des Terres Rares, CNRS No. 180, Paris, Grenoble, 1969, p. 149 (to be published).
[2] E. D. Jones, J. Phys. Chem. Solids **29**, 1305 (1968).
[3] M. Ball, W. P. Wolf, and A. F. G. Wyatt, Clarendon Laboratory Technical Report No. AF61(052)-125, 1963 (unpublished).
[4] W. J. Nicholson and G. Burns, Phys. Rev. **133**, A1568 (1964).
[5] D. T. Edmonds and A. J. Lindop, J. Appl. Phys. **39**, 1008 (1968).
[6] K. C. Brog, W. H. Jones, Jr., and C. M. Verber, Phys. Letters **20**, 258 (1966).

We discuss here in more detail previously reported[7] results of Tm^{169} and Al^{27} NMR measurements on TmAlG. The Tm^{169} NMR, which was studied only below 4°K, yields the orthorhombic magnetic-susceptibility tensor which is considerably more anisotropic than for TmGaG. From the paramagnetic shifts of the Al^{27} resonance, we obtain the temperature dependence of the susceptibility tensor components between 1.5 and 300°K. The quadrupolar splittings of the Al^{27} resonance lines yield the axially symmetric electric field gradients (efg's) at the aluminum *a* and *d* sites. The unshielded efg's, calculated using the Sternheimer antishielding factor, are compared with corresponding values for other aluminum garnets[5,6] and for iron sites in several iron garnets.[4]

II. EXPERIMENTAL

The crystal was grown from a lead fluoride flux. Its rotation axis was adjusted to within half a degree by the Laue back-reflection technique, and orientation relative to the magnetic field was determined to similar accuracy by examination of the NMR spectra. The magnet system was a Varian 12-in. electromagnet with Fieldial regulation. A Varian wide-line spectrometer was used for frequencies up to 16 MHz, and a similar type of spectrometer was used at higher frequencies. An electronic counter was used to monitor the frequency. All resonant magnetic fields were calibrated using reference samples of D_2O, or a water solution of $Al_2(SO_4)_3$ in which the Al^{27} resonances exhibited the published gyromagnetic ratio as found by checking against the deuteron resonance in D_2O. The incremental Al^{27} diamagnetic shift is considered to be negligible.

The Tm^{169} spectra were obtained at 25 MHz, though other frequencies were used initially to identify several false resonance lines which did not shift field with changing frequency. The Al^{27} spectra at 4°K were obtained using frequencies of 6, 8, 16, and 23 MHz to look for effects of saturation of the thulium magnetization. Room-temperature measurements were made at 11 and 16 MHz, while 20 MHz was used at 1.5, 27, 76, 192, and 232°K. The latter four temperatures were attained by immersing the crystal in baths of liquid Ne, N_2, $CClF_3$, and $CHClF_2$, respectively, while liquid-helium baths at atmospheric and at reduced pressure, respectively, were used to attain 4 and 1.5°K.

III. Tm^{169} NMR RESULTS

The spin of Tm^{169} is $\frac{1}{2}$, thus, this nucleus has no electric quadrupole interaction. The thulium resonance shows the existence of large paramagnetic shifts, with $\Delta H/H_0$ varying from 2.50 to 95.34 as a function of crystal orientation relative to the applied magnetic field H_0 giving resonance. The paramagnetic shifts at Al^{27} sites do not exceed 0.04, and agree quite well with predictions based on point dipoles at the Tm^{169} sites. The paramagnetic shifts at a thulium nucleus due to all the other Tm^{3+} ions should be somewhat smaller than 0.04, because the nearest Tm^{3+} neighbors are farther away than for Al^{27}. Accordingly, we make two assumptions which should be accurate to better than 1%: (1) ΔH at a Tm^{169} nucleus is the hyperfine field H_{hf} caused by that Tm^{3+} ion; (2) the bulk paramagnetic susceptibility χ is due only to the Tm^{3+} ions. The first assumption allows us to write

$$\mathbf{H}_L-\mathbf{H}_0\equiv\Delta\mathbf{H}=\mathbf{H}_{hf}=A\mathbf{H}_0\cdot\{\chi\}\,, \tag{1}$$

where A is a magnetic hyperfine interaction constant, $\{\chi\}$ is the magnetic-susceptibility tensor for a particular Tm^{3+}-ion site, and $H_L=2\pi\nu/\gamma$ is the total field at the nucleus at the resonant frequency ν. Here, $|\gamma/2\pi|=0.346$ kHz/G is the Tm^{169} nuclear gyromagnetic ration, *uncorrected* for diamagnetism. In general, $\mathbf{H}_L$ is not collinear with $\mathbf{H}_0$, but for applied field H_{0i} parallel to the ith axis of the diagonalized susceptibility tensor, Eq. (1) reduces to the scalar equation $H_L-H_{0i}=AH_{0i}\chi_i$. Then, the three χ_i can be found by measuring the three values of H_{0i} if the value of A is known.

We obtain Tm^{169} NMR spectra for various angles of rotation ϕ about a ⟨110⟩ rotation axis perpendicular to H_0, with $\phi=0°$ for H_0 parallel to a ⟨100⟩ direction and 90° for H_0 parallel to a ⟨110⟩ direction. For the six nonequivalent thulium sites, one of which is shown in Fig. 1, the χ_1 axes lie in the three ⟨100⟩ directions, while the χ_2 axes lie in the six ⟨110⟩ directions, as do the χ_3 axes. Then, from Eq. (1), the applied fields giving resonance are found to be

$$H_0=H_L[(1+A\chi_1)^2\cos^2\phi+(1+A\chi_2)^2\sin^2\phi]^{-1/2} \tag{2}$$

$$=2H_L[2(1+A\chi_1)^2\sin^2\phi+(1+A\chi_2)^2(\sqrt{2}\cos\phi+\sin\phi)^2+(1+A\chi_3)^2(\sqrt{2}\cos\phi-\sin\phi)^2]^{-1/2}, \tag{3}$$

and also the two expressions for H_0 obtained by interchanging χ_2 and χ_3. A comparison of the applied fields giving resonance with those predicted from Eqs. (2) and (3) is made in Fig. 2. Two of the curves merge at $\phi=90°$, as predicted by Eq. (3). The other two curves merge only at 0°, and the value of $A\chi_1$ is easily obtained from the H_0 of 20.658 kOe at this point, using Eq. (2). Also obtained from Eq. (2) for $\phi=90°$ are $A\chi_2$ and $A\chi_3$, which correspond to applied fields of 0.750 and 11.644 kOe, respectively. This distinction of χ_2 from χ_3 cannot be made on the basis of the Tm^{169} NMR data, but can be made quite convincingly by comparing measured Al^{27} paramagnetic shifts with those predicted from Tm^{3+} dipole sums using both choices for χ_2 and χ_3, as will be shown in Sec. IV. These $A\chi_i$ are used in Eqs. (2) and (3) to obtain the solid lines, which fit the data

[7] E. D. Jones and V. H. Schmidt, J. Appl. Phys. **40**, 1406 (1969).

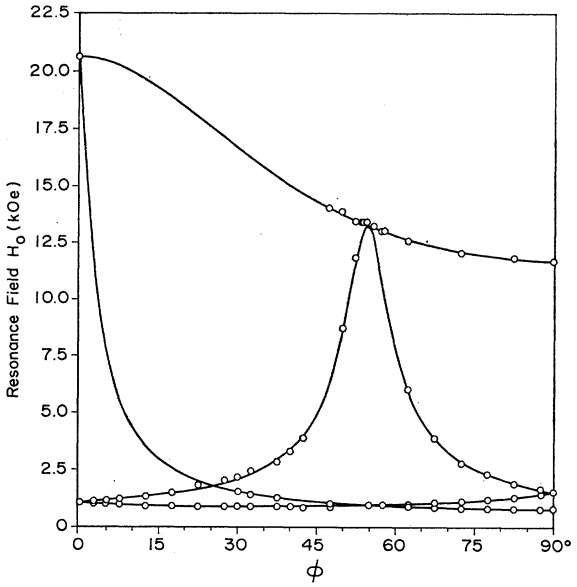

FIG. 2. Angular dependence of the Tm^{169} NMR fields $\mathbf{H}_0$ in the (110) plane for $\nu=25.000$ MHz and $T=1.5$°K. The [100] and [110] directions are given by $\phi=0°$ and $\phi=90°$, respectively. The three resonance fields for $\mathbf{H}_0$ along the χ_1, χ_2, and χ_3 susceptibility tensor axes are 20.658, 0.750, and 11.644 kOe, respectively. The open circles are the measured NMR data and the solid lines are the calculated values.

points very well. In those sections lacking data points, the lines were too broad to be observable.

A comparison of the Tm^{3+} magnetic-susceptibility tensors for TmAlG and TmGaG is shown in Table I. The hyperfine interaction constant $A=172.5\pm3.7$ emu/g ion is obtained from Tm^{169} NMR studies[1] in TmP, TmAs, and TmSb and similar studies[2] in TmGaG. In terms of the more conventional definition for the hyperfine coupling constant of $a\mathbf{I}\cdot\mathbf{J}$, $(a^{169}/h)=-(389\pm4)$ MHz.[8] There is a great difference in the susceptibility tensors for Tm^{3+} in the two materials, with the tensor for TmAlG showing extreme anisotropy. This anisotropy, and its dependence on the nonrare-earth cation, make these materials exceptions to the rule[9] that hyperfine interactions for rare-earth ions are only weakly dependent on the environment. The agreement between the calculated and measured susceptibility for TmAlG as shown in Table I is quite good.

A comparison of the measured hyperfine interaction constant A with a calculated value has been made previously[2] for TmGaG and is presented here in greater detail. One can solve for A in Eq. (1), substituting $-N_A g_J\beta\mathbf{J}/\mathbf{H}_0$ for $\{\chi\}$, where N_A is Avogadro's number, $g_J=7/6$ is the Lande g factor for the $^3H_6$ ground state of the Tm^{3+} ion, β is the Bohr magneton, and $\hbar\mathbf{J}$ is the average total electronic angular momentum for the ion.

[8] W. P. Wolf, M. Ball, M. T. Hutchings, M. J. M. Leask, and A. F. G. Wyatt, J. Phys. Soc. Japan Suppl. B-1 **17**, 443 (1962).

[9] A. J. Freeman and R. E. Watson, in *Magnetism*, edited by G. T. Rado and H. Suhl (Academic Press Inc., New York, 1965), Vol. IIA.

The relation $A=\mathbf{H}_{\rm hf}/N_A g_J\beta\mathbf{J}$ is obtained, in which we substitute

$$\mathbf{H}_{\rm hf}=-2\beta\sum_i\frac{\mathbf{l}_i-\mathbf{s}_i}{r_i^3}+\frac{3(\mathbf{r}_i\cdot\mathbf{s}_i)\mathbf{r}_i}{r_i^5}+\frac{2\delta(\mathbf{r}_i)\mathbf{s}_i}{3r_i^3}. \quad (4)$$

The last term is the contact contribution, which Freeman and Watson[9] estimate as $\mathbf{H}_c\simeq+90$ kOe $(g_J-1)\mathbf{J}$. This term is only about 1% as large as the orbital and spin dipolar contributions. Following Elliott and Stevens,[10] we define

$$\mathbf{N}=\sum_i\left[\mathbf{l}_i-\mathbf{s}_i+\frac{3(\mathbf{r}_i\cdot\mathbf{s}_i)\mathbf{r}_i}{r_i^2}\right]\equiv\langle\mathbf{J}\|N\|J\rangle\mathbf{J}, \quad (5)$$

and write the first two terms of Eq. (4) as $-2\beta\langle r^{-3}\rangle\mathbf{N}$, thereby defining the weighting factor for the average, $\langle r^{-3}\rangle$. The operator equivalent factor $\langle J\|N\|J\rangle$ for Tm^{3+} is 7/9. With these substitutions made in Eq. (4), we obtain

$$A=[2\langle r^{-3}\rangle\langle J\|N\|J\rangle-90\text{ kOe}(g_J-1)/\beta](N_A g_J)^{-1}. \quad (6)$$

The value of A based on the TmGaG bulk susceptibility[3] gives $\langle r^{-3}\rangle=11.7\pm0.2$ a.u., in good agreement with the value 11.7 ± 0.1 a.u. found from Tm^{169} NMR measurements[1] in TmP, TmAs, and TmSb.

IV. Al^{27} NMR RESULTS

A. Analysis of Al^{27} Spectra

The thulium resonance is unobservable above approximately 20°K, so the temperature dependence of the Tm^{3+} magnetic susceptibility was obtained from Al^{27} NMR measurements of the paramagnetic shifts due to the thulium ions. The aluminum NMR also yielded the quadrupolar coupling constants $|e^2qQ/h|$ at the aluminum sites. The a site coupling constant is small enough so that only first-order terms in the quadrupolar perturbations of the Zeeman levels are important, but, for the d site, the second-order terms are important and the third-order terms are not negligible in some instances. Accordingly, we had to use the

TABLE I. Comparison of single-ion and bulk paramagnetic susceptibilities in emu/g ion for TmAlG and TmGaG.

	TmAlG (1.5°K)	TmGaG (4°K)
χ_1	0.014	0.057[a]
χ_2	0.551	0.142 or 0.080[a]
χ_3	0.030	0.080 or 0.142[a]
$\frac{1}{3}\Sigma\chi_i$	0.198[b]	0.093[b]
bulk χ	0.19[c]	0.093±0.001[d]

[a] Reference 2.
[b] Based on A found from bulk χ and Tm^{169} NMR in TmGaG.
[c] Reference 8; measured at 4°K.
[d] Reference 3.

[10] R. J. Elliott and K. W. H. Stevens, Proc. Roy. Soc. (London) **A218**, 553 (1953).

following rather complicated analysis to separate the paramagnetic and quadrupolar effects on the Al^{27} NMR spectra.

The Al^{27} a and d sites have axial symmetry, so we were able to use the following expressions for transition frequencies developed by Pound[11] and corrected by Volkoff,[12] which apply to spin-$\frac{5}{2}$ nuclei in an axially symmetric efg:

$$\begin{aligned}
\nu(\pm\tfrac{5}{2},\pm\tfrac{3}{2}) &= \nu_0(1+K)\{1\pm(3z^2-1)p \\
&\quad +\tfrac{1}{4}y^2(33z^2-1)p^2\pm\tfrac{1}{32}y^2[240y^2z^2 \\
&\quad -(285z^2+3)(3z^2-1)]p^3+\cdots\}, \\
\nu(\pm\tfrac{3}{2},\pm\tfrac{1}{2}) &= \nu_0(1+K)\{1\pm\tfrac{1}{2}(3z^2-1)p \\
&\quad +\tfrac{1}{16}y^2(5-21z^2)p^2\pm\tfrac{1}{64}y^2[(225z^2-33) \\
&\quad \times(3z^2-1)-480y^2z^2]p^3+\cdots\}, \\
\nu(\tfrac{1}{2},-\tfrac{1}{2}) &= \nu_0(1+K)\{1+\tfrac{1}{2}y^2(1-9z^2)p^2 \\
&\quad +\text{fourth-order term}+\cdots\}.
\end{aligned} \tag{7}$$

Here, $p=\nu_Q/\nu_0(1+K)$, $\nu_Q\equiv|3e^2qQ/20h|$ is the splitting between adjacent lines for magnetic field along the efg axis, $\nu_0(1+K)$ is the resonant frequency in the absence of quadrupolar interactions for the field $H_0(1+K)$, which is the sum of the applied field H_0 and the paramagnetic shift KH_0, and y and z are the sine and cosine, respectively, of the angle between the efg axis and the magnetic field $H_0(1+K)$ at the nucleus. Since K is smaller than 0.04 even at 1.5°K, if the Tm^{3+}-ion dipolar field components perpendicular and parallel to H_0 are comparable, the perpendicular components contribute negligibly to the paramagnetic shift magnitudes. They have a greater effect on the field direction, thus, changing y and z in Eqs. (7), but in the worst case of 6MHz and 1.5°K, the error caused by our neglect of the perpendicular components is only of order 1%.

We measured at fixed frequency ν the five applied fields H_0 giving resonance for each Al^{27} site. Equations (7) are rewritten in terms of these H_0's by multiplying them by $H_0/\nu_0\equiv 2\pi/\gamma=0.9014$ G/kHz. They assume the form

$$\frac{2\pi\nu}{\gamma}=H_0(1+K)\left[1\pm C_1\frac{H_Q}{H_0(1+K)}+C_2\left(\frac{H_Q}{H_0(1+K)}\right)^2 \pm C_3\left(\frac{H_Q}{H_0(1+K)}\right)^3+\cdots\right], \tag{8}$$

where the C_j are the coefficients of p^j in Eqs. (7), and $H_Q\equiv 2\pi\nu_Q/\gamma$. The two unknowns in Eq. (8), H_Q and K, govern the quadrupolar and paramagnetic shifts, respectively. The temperature dependence of H_Q is weak, while K decreases rapidly with increasing temperature over a considerable temperature interval. There is some evidence for field dependence of K caused by saturation of the Tm^{3+}-ion magnetization at low temperature and high field. Although our crystal is not symmetric about the rotation axis, the orientation dependence of K showed no evidence of demagnetization effects.

The paramagnetic shifts at the Al^{27} sites at 1.5°K are predicted quite well by assuming point dipoles $\mathbf{H}\cdot\{\chi\}/N_A$ at the thulium sites. The axial symmetry at the Al^{27} sites causes the paramagnetic shift due to such dipolar fields to have orientation dependence

$$K(z)=K_\perp+(K_{\parallel}-K_\perp)z^2, \tag{9}$$

where $K_\perp$ and $K_{\parallel}$ correspond, respectively, to H_0 perpendicular and parallel to the symmetry axis. We assume dipolar fields and accordingly need only four experimentally determined parameters to describe the paramagnetic shifts, namely, $K_\perp$ and $K_{\parallel}$ for the a and d sites. To obtain these parameters we rotated the crystal about a particular ⟨110⟩ axis, which we arbitrarily label $[1\bar{1}0]$, and obtained spectra for H_0 along [001], [112], [111], and [110]. As indicated in Table II, this choice of orientations allows H_0 to become both parallel ($z^2=1$) and perpendicular ($z^2=0$) to the a_1 and d_1 site axes, and perpendicular to the a_2 and d_2 site axes.

Except for the a sites at liquid-helium temperatures, we were able to obtain the quintet of lines from each site for orientations having the site axis parallel to H_0. Such spectra are particularly useful because, as seen from Eqs. (7), there are no second- or higher-order quadrupolar shifts. Accordingly, if at least two lines of the quintet do not overlap other lines, their resonant fields yield both H_Q and $K_{\parallel}$ directly from Eq. (8). Knowing H_Q, we then calculated the first-, second-, and third-order shifts for H_0 perpendicular to the efg axis and assumed for $K_\perp$ the value giving best agreement between the measured and calculated resonant fields. We then predicted values of H_0 for the remaining lines using Eqs. (8) and (9), and adjusted H_Q, $K_{\parallel}$, and $K_\perp$ when necessary to improve agreement between calculated and measured values of H_0.

The general form of the spectra, ignoring paramagnetic shifts and including only first-order quadrupolar shifts, is shown in Fig. 3. The a and d sites give no splitting at 0° and 54.7°, respectively, because from Table II the factor $3z^2-1$ governing first-order splitting

TABLE II. Square of cosine of angle between H_0 and Al^{27} site symmetry axis (z^2) for four orientations about $[1\bar{1}0]$ rotation axis.

Site type	Site axis	Rotation angle ϕ and H_0 direction 0° [001]	35.3° [112]	54.7° [111]	90° [110]
a_1	[111]	1/3	8/9	1	2/3
a_1	$[11\bar{1}]$	1/3	0	1/9	2/3
a_2	$[1\bar{1}1]$	1/3	2/9	1/9	0
a_2	$[\bar{1}11]$				
d_1	[001]	1	2/3	1/3	0
d_2	[010]	0	1/6	1/3	1/2
d_2	[100]				

[11] R. V. Pound, Phys. Rev. **79**, 685 (1950).
[12] G. M. Volkoff, Can. J. Phys. **31**, 820 (1953).

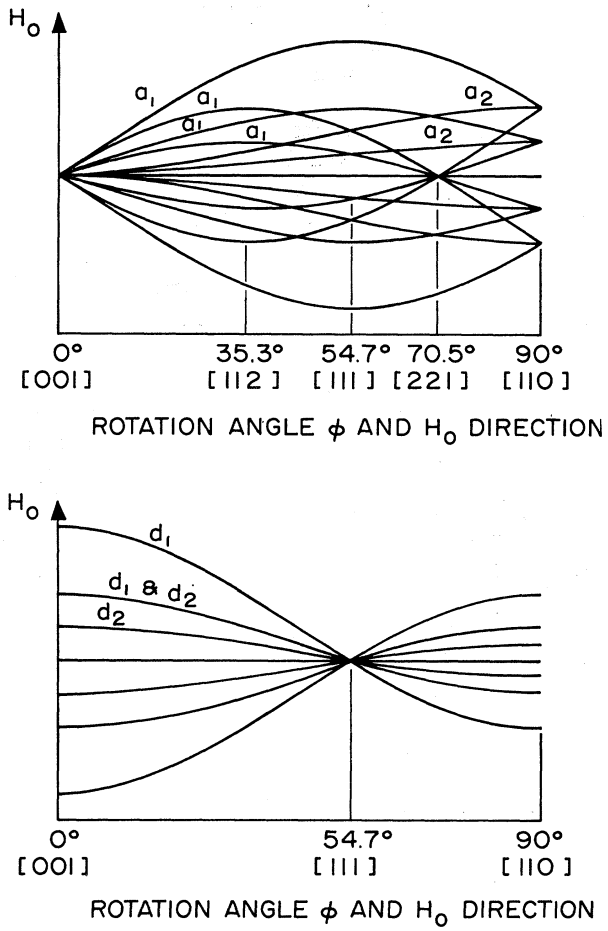

FIG. 3. General form of Al^{27} NMR spectra for rotation about [1$\bar{1}$0] axis. Paramagnetic shifts are ignored and only first-order quadrupolar splittings are included. Lines are labeled according to the site responsible for them.

in Eqs. (7) is zero. The efg at the d sites is large enough so that the second-order quadrupolar interaction gives three lines at 54.7°, but second-order effects on the a-site spectrum are negligible. Figure 3 shows that the d_2 sites have half the splitting of the d_1 sites at all orientations, giving seven lines of which three are degenerate. Second-order quadrupolar shifts separate these degenerate lines in some cases, and at low temperature, the paramagnetic shifts cause even greater separation. At low temperature, the paramagnetic shifts also lift the degeneracy of the a_1 and a_2 quintets for $\phi=90°$, because the K's for these sites differ since the site axes make different angles with H_0.

At liquid-helium temperatures, the resonances become so broad that lines of the a-site quintets generally cannot be resolved, but the a_2 sites give an observable broad line because their spectra have double strength and small splitting. We plotted H_0 for this line against z^2, fit a straight line as predicted by Eq. (9) to the experimental points, and extrapolated to find H_0 for $z=1$, from which K_{11} was determined.

TABLE III. Measured Al^{27} paramagnetic shifts as percentage of applied field H_0, compared with shifts calculated from dipole sums based on Tm^{3+}-ion susceptibilities noted below.

Temperature (°K)	Site and H_0 angle with site axis: a 0°	a 90°	d 0°	d 90°
1.5	−1.41±0.20	2.16±0.10	−3.95±0.10	−3.01±0.30
a	−1.58	1.72	−3.68	−2.83
b	7.86	−2.95	1.02	−0.47
4	−1.33±0.20	2.05±0.10	−3.81±0.10	−2.90±0.20
27	−1.03±0.05	1.72±0.05	−2.84±0.05	−2.26±0.15
76	−0.22±0.05	0.61±0.05	−1.03±0.05	−1.02±0.06
192	0.26±0.03	0.04±0.03	−0.06±0.03	−0.40±0.03
232	0.28±0.03	−0.02±0.03	0.06±0.03	−0.29±0.03
297	0.28±0.01	−0.02±0.02	0.12±0.01	−0.22±0.01
c	0.392	−0.196	0.404	−0.202

[a] Calculated from 1.5°K Tm^{3+} χ tensor (Table I and Fig. 1).
[b] Calculated from 1.5°K Tm^{3+} χ tensor with χ_2 and χ_3 values interchanged.
[c] Calculated from free Tm^{3+} ion χ ($7.15T^{-1}$ emu/g ion).

B. Tm^{3+} Susceptibility from Al^{27} Paramagnetic Shifts

The paramagnetic shifts at the Al^{27} sites are plotted as functions of temperature in Fig. 4. As shown in Table III, the shifts at 1.5°K agree quite well with the shifts calculated for point dipoles $\mathbf{H}_0\cdot\{\chi\}/N_A$ at the thulium sites, where $\{\chi\}$ is the Tm^{3+}-ion susceptibility tensor obtained from Tm^{169} NMR. The shifts were calculated using a dipole sum program which summed the dipolar field components parallel to H_0 from all Tm^{3+} ions within a radius of 100 Å of the aluminum nucleus.

Table III shows that interchanging the axes of the χ_2 and χ_3 components of the susceptibility tensor from those shown in Fig. 1 gives calculated shifts which do

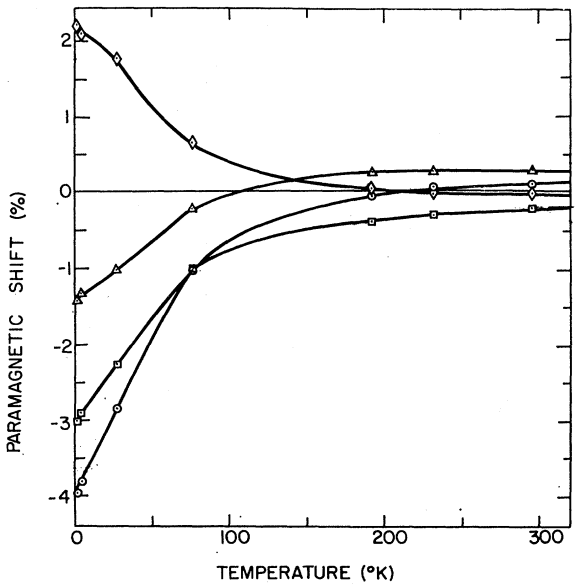

FIG. 4. Temperature dependence of the Al^{27} paramagnetic shifts $\Delta H/H_0$. The a- and d-site shifts for H_0 parallel to the site axes are labeled △ and ○, respectively, while the perpendicular shifts are labeled ◇ and □.

TABLE IV. Comparison of thulium-ion susceptibility tensor components in emu/g ion calculated from Al^{27} paramagnetic shifts and obtained at 1.5°K from Tm^{169} NMR.

Temperature (°K)	Tm^{169} NMR values	Paramagnetic shift omitted in calc χ			
		$K_{\perp a}$	$K_{\parallel a}$	$K_{\perp d}$	$K_{\parallel d}$
1.5	0.014	0.012	0.019	0.143	−0.006
4		0.011	0.018	0.130	−0.050
27		0.014	0.022	0.160	−0.062
76	χ_1	0.015	0.018	0.074	−0.016
192		0.017	0.018	0.040	0.005
232		0.016	0.017	0.035	0.006
297		0.015	0.016	0.040	0.002
1.5	0.551	0.586	0.590	0.999	0.621
4		0.565	0.568	0.938	0.596
27		0.438	0.442	0.899	0.477
76	χ_2	0.192	0.193	0.377	0.207
192		0.066	0.067	0.139	0.073
232		0.047	0.047	0.107	0.052
297		0.034	0.035	0.113	0.041
1.5	0.030	0.053	−0.020	0.011	0.090
4		0.053	−0.013	0.105	0.086
27		0.039	−0.043	0.103	0.080
76	χ_3	0.030	−0.003	0.056	0.047
192		0.029	0.016	0.039	0.035
232		0.026	0.015	0.034	0.031
297		0.023	0.009	0.034	0.030

not agree even qualitatively with the measured shifts at 1.5°K. Thus, the aluminum NMR results have removed the uncertainty in assignment of directions for the χ_2 and χ_3 axes.

The room-temperature paramagnetic shifts are compared in Table III with those calculated from dipole sums based on the free-ion susceptibility $\chi=C/T$, where C is the Curie constant $N_A J(J+1)g_J^2\beta^2/3k=7.15$ emu °K/g ion. There is some qualitative agreement between the measured and calculated shifts. However, the isotropy of the free-ion susceptibility forces the calculated shifts to obey $K_{\parallel}+2K_{\perp}=0$, while the corresponding measured sums differ considerably from zero, so the thulium-ion susceptibility is not isotropic at room temperature.

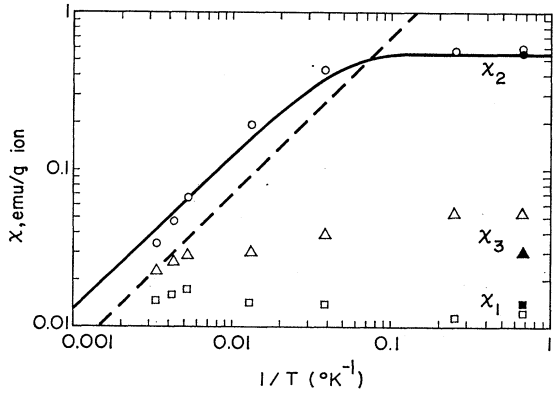

FIG. 5. Temperature dependence of thulium-ion susceptibility components calculated from the $K_{\parallel a}$, $K_{\parallel d}$, and $K_{\perp d}$ Al^{27} paramagnetic shifts (open symbols) and obtained at 1.5°K from Tm^{169} NMR (filled symbols), compared with susceptibilities for a free Tm^{3+} ion (broken line) and for a two-level system with 32-cm^{-1} separation (solid line).

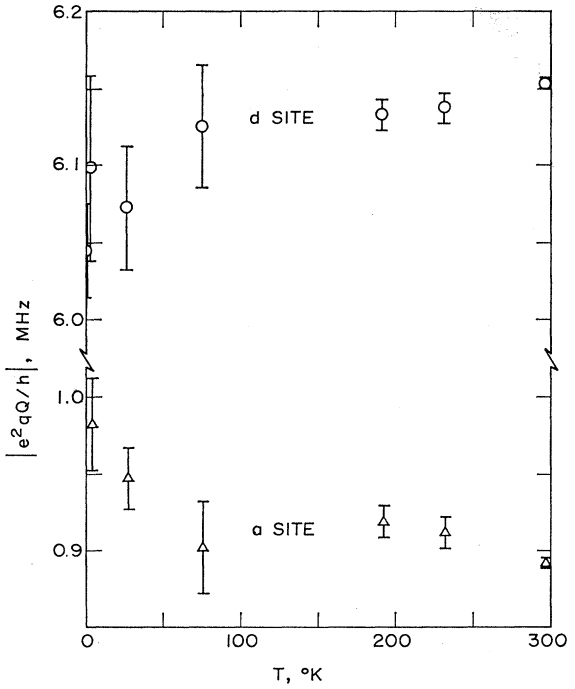

FIG. 6. Temperature dependence of Al^{27} quadrupolar coupling constants.

Because the shifts calculated from the susceptibility at 1.5°K differ only by about 10% from the measured paramagnetic shifts, it seems reasonable that the susceptibility could be calculated to comparable accuracy from the shifts measured at temperatures for which the susceptibility cannot be obtained from Tm^{169} NMR. We have calculated the three components of the susceptibility tensor from the four equations $K_i=B_{i1}\chi_1+B_{i2}\chi_2+B_{i3}\chi_3$, where the K_i are the four measured quantities $K_{\parallel}$ and $K_{\perp}$ for the a and d sites, and the B_{ij} are parameters obtained from the dipole sums. We obtain four values for each tensor component by omitting each equation in turn and solving for the χ_i from the remaining three equations. The results are shown in Table IV. The magnitudes of the four values for each susceptibility component bear the same general relation with respect to each other from 1.5°K to room temperature, indicating that the deviations of the measured paramagnetic shifts from those calculated using the point-dipole approximation have a cause which is effective over this entire temperature range. These deviations probably occur because the nearest thulium ions produce fields at the Al^{27} sites which differ appreciably from point dipole fields, although the possibility of a transferred hyperfine interaction is not ruled out.

Table IV shows that the best agreement with the susceptibility found from Tm^{169} NMR at 1.5°K occurs for the χ_i values found by omitting the a-site $K_{\perp}$ equation, and probably these values are close to the actual susceptibility at higher temperature also. A log-log plot of these susceptibility component values against

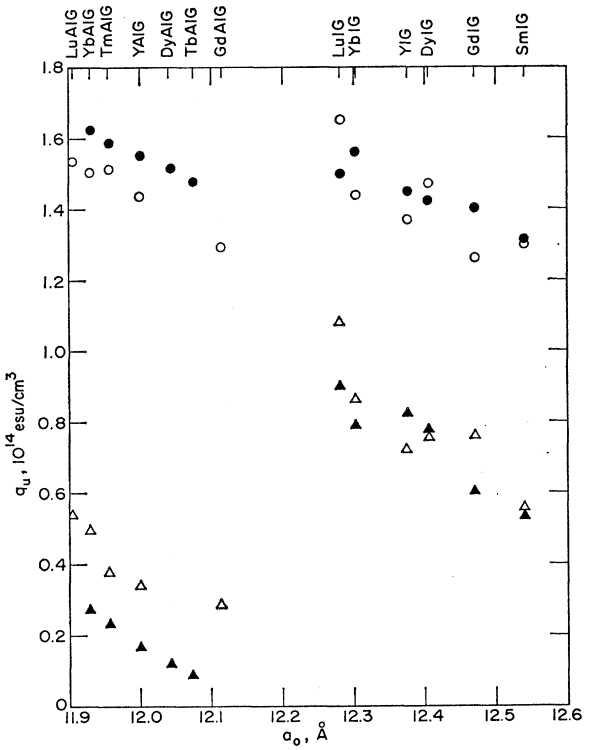

FIG. 7. Calculated (open symbols) and measured (filled symbols) values of the unshielded efg q_u at aluminum and iron a sites (triangles) and d sites (circles) in various garnets as a function of lattice constant. References and methods of obtaining these values are given in Table V and Sec. IV C.

T^{-1} is shown in Fig. 5. The temperature independence and large magnitude of χ_2 at low temperature indicate the existence of a state located a small energy δ above a nondegenerate ground state. The energy-level scheme is not known, so to get an idea of the magnitude of δ, we assume that the first excited state also is nondegenerate and ignore higher states. This simple case of Van Vleck paramagnetism has susceptibility $\chi=\chi_0 \tanh(\delta/2kT)$, where $\chi_0=2N_A|\langle s|\mu_z|0\rangle|^2/\delta$ involves the nondiagonal matrix element of the magnetic moment operator μ_z. This susceptibility, with $\chi_0=0.551$ emu/g ion and $\delta/k=46°$K ($\lambda^{-1}=32$ cm^{-1}), is compared in Fig. 5 with the χ_2 points.

Second-order perturbation theory applied to the foregoing two-level model predicts a saturation effect $\Delta\chi_2/\chi_2=-\frac{1}{4}\chi 2H_0^2/N_A\delta=-0.358\times10^{-10}H_0^2$, an order of magnitude too small to be seen with our experimental accuracy. The paramagnetic shifts measured at 4°K for fields up to 21 000 G show some tendency to decrease with increasing field, but not enough to establish the existence of saturation.

C. Al^{27} Quadrupolar Coupling Constants

The temperature dependences of the quadrupolar coupling constants $|e^2qQ/h|$ are shown in Fig. 6. The a-site coupling constant decreases from 0.98±0.03 MHz at 4°K to 0.892±0.005 MHz at 300°K, while the d-site coupling constant apparently increases from 6.10±0.06 to 6.155±0.005 over the same temperature range. The experimental errors at low temperature are larger because of the increased linewidth.

The a-site coupling constant decrease with temperature is considerably faster than would occur if the charge distribution expanded uniformly with temperature, for any reasonable coefficient of thermal expansion. If a model having temperature-independent charges at the nuclear sites is used to calculate the efg at the a site, the temperature dependence of the efg must be ascribed mainly to the oxygens, because as Burns[13] has pointed out, the crystal symmetry is such that if the same charge (such as $3e$) is assigned to both the Tm^{3+} and Al^{3+} sites, the efg's contributed by the Tm^{3+} and Al^{3+} ions will cancel. Since our lattice sum shows that the greater part of the efg contributed by point charges at oxygen sites is due to the nearest oxygens for both a and d sites, we believe that the decrease in efg is due mainly to a decrease with increasing temperature in the distortion of the oxygen octahedron surrounding the a site.

For the aluminum d sites, the efg's contributed by the thulium and aluminum ions do not cancel. These ions form a lattice which must expand exactly as the unit cell expands, giving an efg contribution that decreases with increasing temperature. The oxygens, however, can move relative to the unit cell as temperature changes. Accordingly, an explanation in terms of this point-charge model of the d-site efg *increase* with increasing temperature requires a relative change in oxygen position, which probably involves an increase in distortion of the oxygen tetrahedron surrounding the d site.

A comparison of these results with coupling constants for other aluminum garnets and for iron garnets is made in Fig. 7 and Table V. The unshielded field gradient $q_u=q/(1-\gamma_\infty)$ is plotted in Fig. 7 against lattice parameter, where we use for the Sternheimer antishielding correction $1-\gamma_\infty$ the values 3.59 given by Das and Bersohn[14] for Al^{3+} and 10.14 given by Sternheimer[15] for Fe^{3+}. For the quadrupole moment Q of Al^{27}, we use the value 0.149 b.[16] For the 14.4-keV excited state of Fe^{57}, we use the value 0.2 b adopted by Nicholson and Burns[4] for their calculation of q_u in six iron garnets; a more recent value is 0.21±0.03 b.[17]

The calculated q_u for the aluminum a sites are based on lattice sums which we performed over all oxygens within a 100 Å radius of the a site, using essentially the same computer program as we used for the magnetic dipole sums. For the d sites, we performed a similar lattice sum for the oxygens and, in addition, used the

[13] G. Burns, Phys. Rev. **124**, 524 (1961).
[14] T. P. Das and R. Bersohn, Phys. Rev. **102**, 733 (1956).
[15] R. M. Sternheimer, Phys. Rev. **130**, 1423 (1963).
[16] G. E. Pake, Ann. Rev. Nucl. Sci. **4**, 33 (1954).
[17] R. Ingalls, Phys. Rev. (unpublished).

positive ion lattice sum results of Burns.[13] Because Table I of Nicholson and Burns[4] shows that the most obvious choice of charges, namely, $3e$ at the iron and rare-earth sites and $-2e$ at the oxygens, gives very poor agreement between measured and calculated coupling constants, we allowed the oxygen charge to be an adjustable parameter and found that a positive value of $1.2e$ gives quite good fit to both the aluminum and iron garnet results, as shown in Fig. 7. To calculate q_u for the iron garnets, we subtracted from Nicholson and Burns's calculated q_u the contribution from the positive ions obtained from Burns's lattice sums to obtain the field gradient contributed by charge $-2e$ at each oxygen, multiplied this contribution by -0.6 and added the positive ion contribution. The lattice constants and oxygen positions used in this calculation are taken from the x-ray studies of Euler and Bruce,[18] with the exceptions that we used Weidenborner's[19] values for GdIG and Morosin's[20] for TmAlG.

In Fig. 7, the regular variation with lattice parameter of q_u and, accordingly, of coupling constant, as pointed out by Edmonds and Lindop,[5] is clearly evident, particularly for the aluminum garnets which benefit from the higher accuracy of NMR measurements. The Al^{27} coupling constants were measured by us for TmAlG, by Edmonds and Lindop for TbAlG, DyAlG, and YbAlG, and by Brog, Jones, and Verber[6] for YAlG. Although yttrium is not a rare earth, the values of q_u for YAlG fit in perfectly with those for the rare-earth garnets. For each of the four series consisting of aluminum and iron a and d sites, the variation of q_u with lattice constant is about the same for the calculated and experimental values. The experimental agreement with the prediction that the q_u for the aluminum a sites are much smaller than for the iron a sites indicates that the a-site coupling constant is governed primarily by distortion of the oxygen octahedron surrounding the a site, since only the oxygens contribute to the calculated a-site efg and the nearest six oxygens give the major part of this contribution.

Our choice of charge $1.2e$ at oxygen sites and $3e$ at positive ions gives agreement with experiment which is surprisingly good for a point-charge model having one arbitrary parameter. We presently cannot explain why best agreement with experiment results from use of a positive charge $1.2e$ for this parameter.

To investigate whether similar point-charge models can predict field gradients in other crystals containing oxygen, we have calculated the efg at the copper nucleus in Cu_2O due to the nearest two oxygens, which contribute the majority of the efg. To obtain agreement with the copper nuclear quadrupole resonance frequencies measured by de Wijn and de Wildt,[21] a charge $\pm 0.9e$ is needed at each of these two oxygens.

TABLE V. Calculated and measured values of the unshielded efg q_u in 10^{14} esu/cm^3 at aluminum and iron sites in various garnets. Calculated q_u are positive; signs for measured q_u are not known. The garnets are listed in order of increasing lattice constant.

Garnet	a site		d site	
	Calc[a]	Meas[b]	Calc[a]	Meas[b]
LuAlG	0.537	...	1.537	...
YbAlG	0.494	0.272	1.503	1.625
TmAlG	0.375	0.230	1.511	1.587
YAlG	0.340	0.162	1.435	1.552
DyAlG	...	0.115	...	1.515
TbAlG	...	0.082	...	1.478
GdAlG	0.286	...	1.294	...
LuIG	1.08	0.90	1.65	1.50
YbIG	0.86	0.79	1.44	1.56
YIG	0.72	0.82	1.37	1.45
DyIG	0.75	0.78	1.47	1.42
GdIG	0.76	0.60	1.26	1.40
SmIG	0.55	0.53	1.30	1.31

[a] Based on positive point charges $3e$ at cations and $1.2e$ at oxygens, for structures reported in Ref. 19 for GdIG, Ref. 20 for TmAlG, and Ref. 18 for the other garnets.
[b] Obtained from measured coupling constants (Ref. 5 for YbAlG, DyAlG, and TbAlG, Ref. 6 for YAlG, and Ref. 4 for iron garnets), using Q of 0.149 and 0.20 b and $1-\gamma_\infty$ of 3.59 and 10.14 for Al^{27} and Fe^{57*} nuclei, respectively.

V. DISCUSSION

The Tm^{169} NMR results at 1.5°K have shown that the thulium ion undergoes an orthorhombic crystal field interaction which is much more anisotropic than in TmGaG. The Tm^{3+} energy-level scheme which gives rise to this unusually strong dependence of $4f$ electron behavior on environment is not known.

The paramagnetic shifts measured at 1.5°K at the Al^{27} sites can be accounted for quite well in terms of dipolar fields from the thulium ions, although the possibility of a transferred hyperfine interaction is not ruled out. The approximate temperature dependence of the thulium magnetic susceptibility tensor components has been calculated from the temperature dependence of the paramagnetic shifts. Near room temperature, the susceptibility shows a tendency to approach the isotropic free-ion susceptibility, so it would be desirable to extend the Al^{27} paramagnetic shift measurements above room temperature to find whether the susceptibility does become isotropic. The large magnitude and the temperature dependence of the χ_2 susceptibility component indicate Van Vleck paramagnetism due to a state some 30 cm^{-1} above the ground state. We cannot obtain complete information on the splittings of the thulium ion $^3H_6$ ground state due to the orthorhombic crystal field because there are nine unknowns in the Hamiltonian.[22] However, our data for the magnitudes

[18] F. Euler and J. A. Bruce, Acta Cryst. **19**, 971 (1965).
[19] J. E. Weidenborner, Acta Cryst. **14**, 1051 (1961).
[20] We are indebted to Dr. B. Morosin for supplying to us in advance of publication his measured values at room temperature: lattice constant = 11.9566 (3)Å, $O_x = -0.0302$ (7), $O_y = 0.0513$ (7), $O_z = 0.1506$ (7).
[21] H. W. de Wijn and J. L. de Wildt, Phys. Rev. **150**, 200 (1966).
[22] W. P. Wolf, in *Proceedings of the International Conference on Magnetism, Nottingham, 1964* (The Institute of Physics and The Physical Society, London, 1965).

and temperature dependence of χ_1, χ_2, and χ_3 can provide a good test of any proposed level scheme.

The temperature dependence of the quadrupolar splittings of the Al^{27} resonance lines indicates a change with temperature in the oxygen configurations, probably involving increased distortion of the AlO_4 tetrahedra with increasing temperature. A low-temperature structure study would show what oxygen position changes occur. The unshielded efg at the aluminum sites in several aluminum garnets and at the iron sites in some iron garnets are predicted quite accurately by a point-charge model having charge $3e$ at each trivalent cation site and *positive* charge $1.2e$ at each oxygen site. It would be of interest to see if similar point-charge models for other crystals require positive charges at oxygen sites.

ACKNOWLEDGMENTS

We wish to thank R. J. Baughman for growing the single crystals, Dr. B. Morosin for supplying x-ray structure data in advance of publication, Dr. A. Narath for providing the dipole-sum computer program, and R. R. Knispel for assistance with computer calculations of efg. One of us (V.H.S.) gratefully acknowledges summer support at Sandia Laboratories under the Association of Western Universities Atomic Energy Commission Faculty Participation Program, and thanks personnel at Sandia Laboratories for their hospitality.

PHYSICAL REVIEW B VOLUME 1, NUMBER 5 1 MARCH 1970

Electron Paramagnetic Resonance of V^{3+} Ions in Zinc Oxide

G. FILIPOVICH, A. L. TAYLOR, AND R. E. COFFMAN*
3M Company, Central Research Laboratories, St. Paul, Minnesota 55101
(Received 28 April 1969; revised manuscript received 22 October 1969)

The paramagnetic resonance of trace amounts of V^{3+} in single-crystal hexagonal zinc oxide is reported. The EPR spectrum is fitted with an axially symmetric spin Hamiltonian with five empirically determined parameters: D, $g_{\parallel}$, $g_{\perp}$, A, and B. The spin-Hamiltonian parameters are interpreted in terms of the Racâh parameter B, the crystal-field parameters Dq, Ds, Dt, and the spin-orbit coupling constant λ. The values of these parameters derived from the EPR data are consistent with a model in which the V^{3+} replaces a Zn^{2+} in a trigonally elongated tetrahedral site. This is in agreement with a recent redetermination of the crystallographic unit-cell parameters of ZnO.

I. INTRODUCTION

THE electron-paramagnetic-resonance (EPR) absorption of V^{3+} in tetrahedral site symmetry has been reported for vanadium in ZnS and ZnTe crystals[1,2] having the cubic zinc sulfide structure. The EPR spectrum of V^{3+} in an eightfold coordinated cubic site has been reported for vanadium in single-crystal CaF_2,[3] having the fluorite structure. In both the fourfold and eightfold cubic coordination, the crystal-field potential has the opposite sign in relation to the crystal-field potential for the sixfold octahedral coordination.[4] The ground state is therefore orbitally nondegenerate with a small amount of mixing of excited orbital momentum states due primarily to the spin-orbit coupling. The ground-state spin degeneracy is not removed in these cases, so the EPR spectra are magnetically isotropic for the cases of tetrahedral symmetry.

The EPR[2] and optical spectra[5] of V^{3+} in single-crystal CdS having the zincite (wurtzite) structure have been reported. The Cd site in this crystal structure is axially distorted because the Cd-S distance along the crystalline c axis is shorter than the other three Cd-S separations in the tetrahedron. These distances were believed, in 1948, to be 2.51 and 2.53 Å, respectively.[5,6] In this paper, we present the results of a study of the EPR of V^{3+} in a Zn-atom subsitutional site in single-crystal ZnO. Recently, the atomic distances in ZnO have been remeasured[7] and show a slight axial elongation of the tetrahedron (Fig. 1). The Zn-O c-axis distance is 1.992 Å, while the other three Zn-O bond distances are each 1.973 Å. According to the data published in 1948,[6] these same dimensions are 1.796 and 2.040 Å, respectively, indicating a large axial compression. This c-axis trigonal distortion partially removes the spin degeneracy of the $^3A_{2g}$ ground state, giving anisotropic EPR spec-

* Present address: Chemistry Department, University of Iowa, Iowa City, Ia. 52240.
[1] W. C. Holton, J. Schneider, and T. L. Estle, Phys. Rev. **133**, A1638 (1964).
[2] G. W. Ludwig and H. H. Woodbury, Bull. Am. Phys. Soc. **6**, 118 (1961); Solid State Phys. **13**, 299 (1962).
[3] M. M. Zaripov, V. S. Kropotov, L. D. Livanova, and V. G. Stepanov, Fiz. Tverd. Tela **9**, 209 (1967) [English transl.: Soviet Phys.—Solid State **9**, 155 (1967)].
[4] J. S. Griffith, *The Theory of the Transition Metal Ions* (Cambridge University Press, Cambridge, England, 1961).
[5] R. Pappalardo and R. E. Dietz, Phys. Rev. **123**, 1188 (1961).
[6] R. W. G. Wyckoff, *Crystal Structures* (Wiley-Interscience Inc., 1949), Vol. I, table p. 31.
[7] S. C. Abrahams and J. L. Bernstein, Acta Cryst. **25**, 1233 (1969).